DUE AVALRS: REMOTE-SENSING DERIVED AVALANCHE INVENTORY DATA FOR DECISION SUPPORT AND HIND-CAST AFTER AVALANCHE EVENTS

Regula Frauenfelder[(1)], Kalle Kronholm[(1)], Rune Solberg[(2)], Siri Øyen Larsen[(2)], Arnt-Børre Salberg[(2)], Jan Otto Larsen[(3)], Heidi Bjordal[(3)]

[(1)]Norwegian Geotechnical Institute, P.O. Box 3930 Ullevaal Stadion, 0806 Oslo, Norway, Email: rf@ngi.no
[(2)]Norwegian Computing Center, P.O. Box 114 Blindern, 0314 Oslo, Norway
[(3)]Norwegian Public Roads Administration, P.O. Box 8142 Dep., 0033 Oslo, Norway

ABSTRACT

Each year, snow avalanches hit populated areas and parts of the transport network in the Norwegian mountain regions, leading to loss of lives and the damaging of buildings and infrastructure. We present the results of a feasibility study on the operation of a service providing the National Public Roads Administration (NPRA) with hind-cast avalanche inventory data on a local-to-regional scale during the course of the winter season, and as soon as possible after major avalanche events. We have explored the use of imagery from high-resolution and very-high-resolution space-borne satellites applying manual mapping and automated image segmentation.

1. INTRODUCTION

Avalanches or high avalanche danger levels are regularly the cause of temporary closures of important national transport corridors. Over the last 10 years pressure on the authorities has increased to keep road closures to a minimum while keeping the safety of the transport corridors at an acceptable level. Due to the size of the Norwegian road network, daily avalanche forecasts during wintertime are issued for specific sections only. While forecasts for avalanche risk management rely mainly on meteorological forecasts, snow cover observations and expert knowledge, satellite-based remote sensing has a large potential in now- and hind-casting. The area covered by remote sensing approaches can be regional to local and stretch over areas where traditionally such measurements are both difficult and time-consuming, or areas that are not accessible at all for in-situ observations.

2. BACKGROUND

2.1. Avalanches

An avalanche (Fig. 1) is a rapid flow of snow down a slope, released by either natural or human triggering. Powerful avalanches have the capability to entrain ice, rocks, trees, and other material on the slope; however avalanches are always initiated in snow, and primarily composed of flowing snow. In mountainous terrain avalanches are among the most serious objective hazards to life and property, with their destructive capability resulting from their potential to carry an enormous mass of snow (and eventually other material) rapidly over large distances. All avalanches share common elements: a trigger which causes the avalanche, a start zone from which the avalanche originates, a slide path along which the avalanche flows, a run out where the avalanche comes to rest, and a debris deposit which is the accumulated mass of the avalanched snow once it has come to rest.

Figure 1. Upper picture: artificially triggered avalanche at Ryggfonn, NGI's avalanche research test site in Grasdalen, Norway (photo by NGI). Lower picture: taxi caught by avalanche on national road Rv609 near Eidsfjorden, Norway on March, 8th, 2010 (photo by Hanne Mjåseth).

Avalanches have a failure layer that propagates the failure. The nature of the failure of the snow pack is used to morphologically classify the avalanche. Slab avalanches are generated when an additional load causes a brittle failure of a slab that is bridging a weak snow layer; this failure is propagated through fracture formation in the bridging slab. Loose snow, point release, and isothermal avalanches are generated when a stress causes a shear failure in a weak interface, either within the snow pack, or at the base. When the failure occurs at the base they are known as full-depth avalanches.

2.2. Field mapping of avalanches

Currently, the detection and mapping of avalanches relies mainly on isolated observations acquired by individuals under field conditions. Consequently, the achieved coverage is rather poor as only events within a restricted region can be recorded. Quite often, only avalanches causing accidents or resulting in heavy damages are mapped. Large parts of the Norwegian mountains are inaccessible to observers, especially during periods of high avalanche danger level. No systematic detection and mapping of avalanches over large areas is carried out today. However, acquisition of such data would be important for verification purposes, e.g., for independent assessment of the accuracy of issued avalanche warnings.

Traditionally, avalanches are mapped in the field by recording certain parameters of the avalanche. The National Public Roads Administration (NPRA) has a special form for the reporting of avalanches (and other gravitational processes) affecting their road network, the so-called R11 form. In this form, the type of observed gravitational process (in the context of this project only 'avalanches' are relevant) is reported, the approximate height between the road and the release area, the depositional volume and the length of the blocked road segment. Additional information such as reporting of damage (no/yes; if any: what type), current weather situation, and imposed road closure measures is also required. Weather information from weather stations may also be reported but is not required. Maps and photographs are linked to the reports where such material is available. The data reported in these forms is punched into a digital database which is periodically mirrored into the national Norwegian database on gravitational processes (www.skrednett.no). However, only avalanches directly affecting roads are registered, i.e., only the location and characteristics of the deposit area are stored, but not of the release area or the avalanche path. However, such information would be crucial in order to, for example, improve models used in avalanche forecasting.

2.3. Remote sensing of avalanche events

Current approaches for remote sensing based avalanche detecting cover quite a broad range of applications both in view of applied techniques, covered scale ranges and used data. Small scale applications are mostly focused on the exploitation of the capabilities of laser scanning [1] or ground-based synthetic aperture radar (SAR) [2]. These approaches are, however, not adequate to cover large areas or for the operational mapping of avalanches.

Traditionally large-scale applications originated from the analysis of aerial imagery [3]. Such data analysis was extremely time-consuming due to analogue image interpretation. Today, feasible applications stem either from semi-automatic classifications of optical imagery, or the interpretation of SAR data. References [4, 5] report on the use of ASAR C-band for avalanche detection, but they also state that the current available satellite systems (mainly C-band SAR that is applicable) are not very well suited for snow-related applications due to the small influence of the dry snow on the microwave signal at C-band. New missions, such as TerraSAR-X and future missions such as CoreH2O [6] have the potential to improve microwave remote sensing of snow on a local scale and in mountainous areas. Recently [7] presented an approach using an air-borne digital scanner (ADS40). Their approach looks promising; however, it requires the availability of such an instrument.

2.4. Current practice

NPRA is responsible for the planning, construction and operation of the national and county-road networks. The objective of NPRA is to develop and maintain a safe, eco-friendly and efficient transport system.

During winter season a major challenge for the NPRA is to maintain the risk level from avalanches on the roads below an acceptable level. In cases where avalanches have closed roads, the challenge is to re-open the roads as soon as possible (within the allowed risk level) to ensure efficient transport corridors.

Before avalanches hit the road the NPRA makes the close/no-close decision based on an avalanche forecast. Avalanche forecast and field evaluations form the basis for decisions made to re-open a road after a closure. In these cases the authorities must obtain a reliable avalanche forecast. For this purpose the NPRA is very interested in a way to evaluate the avalanche forecasts in hind-sight. Observations of avalanches in the nearby terrain are one of the best ways of validating an avalanche forecast.

After an avalanche has hit a part of the road network the goal of the NPRA is to re-open the affected road as fast as possible, while at the same time providing maximum safety for the staff opening the roads and the persons travelling on the affected stretch of road after its re-opening. To this end, NPRA tries to:

(1) Obtain an overview of the problem as soon as possible after the avalanche event. Up to now, such an overview is obtained by either on-site inspection from NPRA's sub-contractors (entrepreneurs) or by carrying out reconnaissance flights over the affected stretch of road with a helicopter if weather permits. This method has the obvious drawbacks that it is dependent on good flight conditions

(weather, light conditions in regions above the polar circle) and that observations can only be made along the flight path.

(2) Once an overview has been gained, the decision on when to re-open the road is taken. NPRA's entrepreneurs are then responsible for the broaching of the affected road segment.

Road closures typically last several hours to a few days. Often re-opening happens earliest the morning after the event due to personnel safety regulations for the involved staff which do not allow for road broaching during the night.

2.5. Brief description of envisaged service

The main objective of the here presented avalRS project is to provide the Norwegian Public Roads Authority (NPRA) with avalanche inventories based on remote sensing data captured briefly after major avalanche events. AvalRS aims to explore if such a service (Fig. 2) is possible and if it could provide decision support during avalanche-imposed road closures and help validate the issued avalanche forecasts. The interest is two-fold:

(a) To obtain information on what has happened after large avalanche events, regardless of aircraft flight conditions.

(b) To obtain spatially distributed avalanche inventory data.

(a) Hind-cast data: Often, helicopter reconnaissance flights after large avalanche events are not possible. In such cases information from space-borne methods would be extremely useful to assess the extent and the magnitude of the event, eventual damage, etc.; (b) Inventory data: The service and its products could also be useful as a mean to improve the existing avalanche warnings. In view of the pending challenge to expand and improve the Norwegian road network, avalanches recorded in areas where such observations are missing, are also of special interest. In this context, not only avalanches hitting the road network are of importance but also avalanches hitting protection structures (both those against avalanches and those against other gravitational processes). An important question is, for example, the question about the effectiveness of such protection structures. If new roads are built it is also important to have information about avalanches in the area of the planned road.

It is expected that climate change will have an influence on avalanche activity, especially that the amount of wet avalanches will increase. To monitor such expected climate change impacts, frequent and regionally distributed avalanche inventory data is crucial. For the inventory, information on the size of the

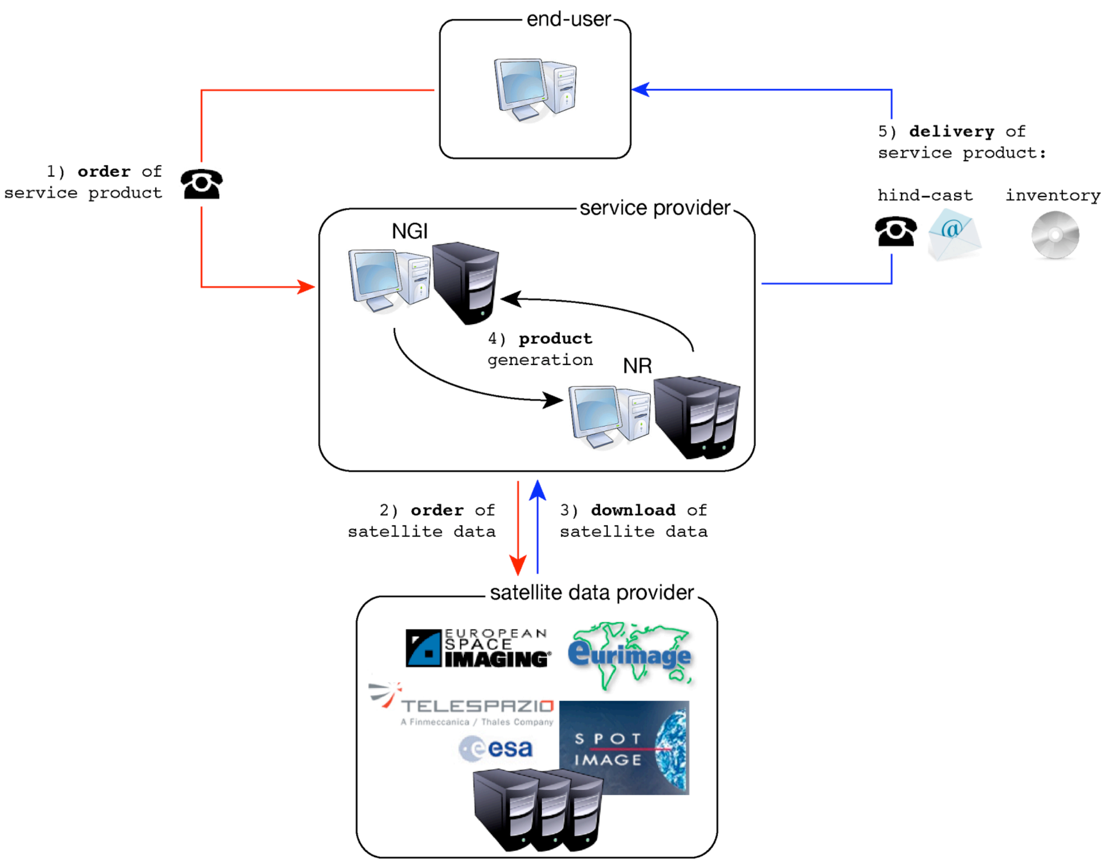

Figure 2. Schematized overview of the service architecture with its flows of request, data and work between end-user, service provider and satellite data provider.

avalanche, the run-out length, the avalanche type (slab, loose snow, point release, etc.) are of interest.

3. DATA AND METHODS

We explored the use of imagery from high-resolution (HR) and very high resolution (VHR) space-borne satellites, applying the following methods: a) manual mapping, b) automated image segmentation, c) automated feature extraction, and d) a combination of b) and c).

Data from four test cases (Fig. 3) were analyzed on an iterative basis:

1. High-resolution (HR) SPOT-2/-4 multi-spectral data from the Tyin area
2. HR SPOT-4 panchromatic data from the Otta area
3. Very-high-resolution (VHR) panchromatic Quick-bird data from the Hellesylt area and the Dalsfjorden area.

Figure 3. Location of the four test sites Tyin, Otta, Hellesylt and Dalsfjorden.

3.1. Detection of avalanches in HR optical satellite data

An avalanche event from 2008 was chosen in a first step: between January 24th and 26th, 2008 several large avalanches blocked large sections of a major regional road ('Fylkesvei' Fv53) for several days (Fig. 4). Ancillary data for this event was available from a helicopter flight undertaken by the NPRA shortly after the event.

Figure 4: Avalanche event in January 2008 in the Tyin area, Central Norway. Avalanches were naturally released in the period from 24.01.2008 to 26.01.2008. Road closure lasted for approx. 3 days. Upper picture: manually recorded avalanche events on and along Fv53 (Map source: NPRA). Lower picture: oblique photograph of a snow avalanche crossing the road. The avalanche had descended from right to left, first crossing the snow drift fence, then the road and finally destroying one building. (Photo by Svein Helge Frækaland, NPRA Region west, 27.01.2008).

SPOT-2 and SPOT-4 data was acquired through a Category 1 proposal. Multi-spectral data from SPOT-2 and SPOT-4 data from after the event was available for the dates of 12.2.2008 and 15.2.2008. These scenes have a spatial ground resolution of 20 m, and three (SPOT-2), respectively four (SPOT-4) multi-spectral bands covering green, red and near-infrared, and green, red, near-infrared and mid-infrared, respectively.

In a first step, the imagery was geo-referenced and integrated into a Geographical Information System (GIS). Secondly, we tried to detect and map the avalanches released during the above event.

The result of this proofed negative: avalanches released during the event were not visually detectable in the available SPOT-2/-4 multi-spectral scenes. The fact that avalanches were not detectable in the available scenes is seen as a combination of two factors: (a) too coarse spatial ground resolution (20 m) of the SPOT-2/-4 multi-spectral imagery; (b) considerable time-lag between the event and the acquisition date of the available scenes of 17 and 20 days, respectively.

The analysis of ancillary data from the Norwegian Meteorological Institute (mainly precipitation data) showed that several small snow fall events had occurred between avalanche releases and the acquisition of the imagery. These individual snow fall events may well have accumulated to a snow cover substantial enough to obscure the original avalanche deposits. While cause (b) certainly didn't favour the detectability of the avalanches, cause (a) is seen as the main issue. Cause (b) would most presumably also have a negative effect on the detectability of the avalanches in the panchromatic channel. However, panchromatic data was not available for this test case.

In order to check if avalanche detection efforts would perform better using SPOT panchromatic data, which has 10 m spatial ground resolution, a scene available for the Otta region – approximately 100 km NE of Tyin (acquired on 15.2.2008) was analysed. In contrast to the scenes from the Tyin area, there is no data available for the Otta area on eventually released avalanches on the date concerned.

As for the multi-spectral data, the panchromatic imagery was geo-referenced and integrated into a GIS, in order to try to detect and map eventually released avalanches.

The unverified expert impression was gained that big, fresh avalanches would be detectable in SPOT-2/-4 panchromatic scenes with favourable illumination conditions. However, efforts to detect (and eventually map) avalanches on the Otta scene did not yield positive results. This is most likely because there were no avalanches to observe. In addition, the illumination of the image was not favourable: north-exposed slopes are mainly in the shadow while south-exposed slopes are "over-illuminated". This makes it nearly impossible to detect eventual avalanche deposits.

3.2. Detection of avalanches in VHR optical satellite data

In earlier projects dealing with automated object detection from satellite images, good results were obtained using an approach consisting of image segmentation into objects, followed by feature extraction and classification. Examples include oil spill detection in SAR images [8], and detection of cultural heritage sites [9] or vehicles [10] in very-high-resolution optical images. A similar approach was, therefore, tested for automated avalanche detection and mapping. Each processing step had to be adjusted to meet the requirements for object recognition of the specific type, which here were avalanches.

Two QuickBird image sections (0.6 m spatial resolution in panchromatic band) from Western Norway were analyzed, one from the Hellesylt area acquired on April 16, 2005 (Fig. 5, cf. Fig. 3 for location), and one from the Dalsfjorden area, acquired on April 3, 2005 (Fig. 6, cf. Fig. 3 for location).

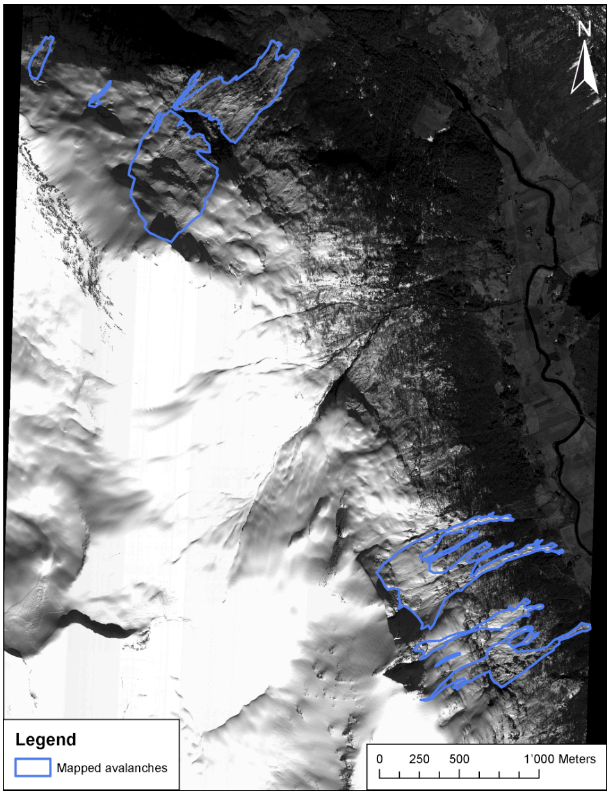

Figure 5. Manually mapped avalanche outlines on a QuickBird image section from the Hellesylt area (acquired on April 16, 2005 (cf. Fig. 3 for location).

A total of 12 avalanches (Hellesylt scene; development data), respectively 19 avalanches (Dalsfjorden area, validation data) were manually delineated. In addition, a digital elevation model (15 m resolution) and forest and agriculture maps were used. Analyses were performed using tools available in and developed by us in ENVI/IDL®, commercial software for processing and analyzing geospatial imagery.

Firstly, the QuickBird images were ortho-rectified using the 15 m resolution digital elevation model (DEM) and manually selected ground control points, using the built-in ENVI function for ortho-rectification. This tool takes into account some sensor specific parameters. Slope and aspect images with resolution corresponding to the panchromatic images were also calculated based on the 15 m DEM. Ortho-rectification using a 25m resolution DEM was also investigated, but due to the very high resolution of the QuickBird images, the accuracy of these results was not sufficient.

Two different segmentation strategies have been tested: texture-based segmentation and segmentation based on directional filters. The two strategies are briefly described in the following (for a more extensive explanation of these approaches, please refer to [11].

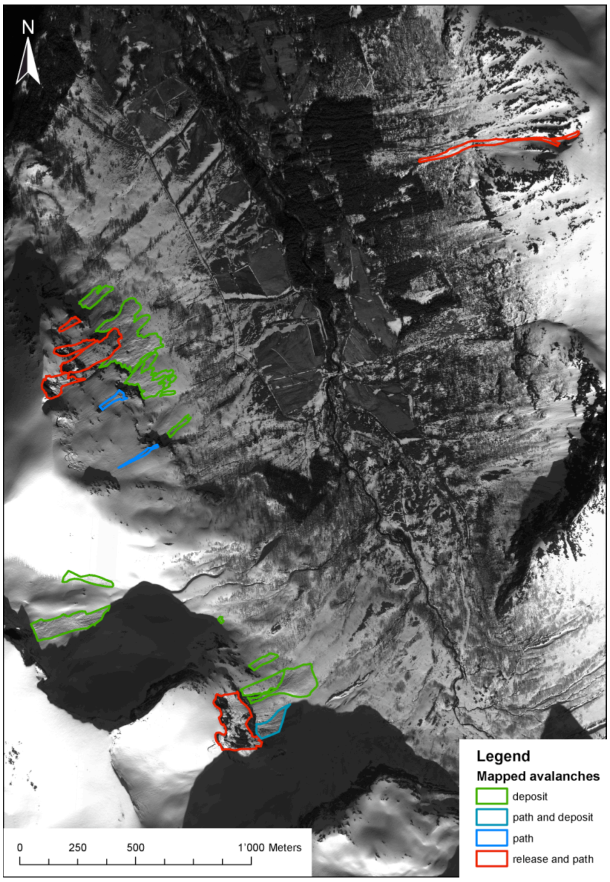

Figure 6. Manually mapped avalanche outlines (differed into deposit areas, path and deposit areas, paths and release and path areas) on a QuickBird image section from the Dalsfjorden area (acquired on April 3, 2005).

3.3. Texture-based segmentation

Texture is one of the important characteristics that make it possible to visually discriminate avalanche affected areas from non-avalanche affected areas in an image. Various textural features were computed from the panchromatic image based on the approach by [12], using the grey-level co-occurrence matrix (GLCM). This matrix describes the grey-level intensity variation between pixels located with a given direction and distance with respect to each other. For many applications, such as the present one, it is natural to compute one GLCM for each pixel neighbourhood in the image, since the image consists of many different textures. The textural features can then be defined in each pixel using a GLCM computed in a neighbourhood centred at this pixel.

3.4. Segmentation using directional filters

Extracting textural features by convolving the image with a given filter is often applied in texture segmentation and classification (cf. e.g., [13, 14]). Typically, a set of convolved images is created by applying filter banks, each with given characteristics (e.g., scale, orientation, frequency, etc.). Then each filtered image is combined into a multi-dimensional image, which is further analyzed to stratify the image into segments with similar texture patterns.

The approach applied here is based on the work by [15]. First, a set of regions of interest (ROIs) is selected, each corresponding to the following texture types or content classes: *avalanche, smooth snow, rugged snow, sparse trees,* and *rock*. Since forest and agriculture masks are available, ROIs corresponding to dense forest and agriculture areas were not selected.

4. RESULTS

4.1. Segmentation based on texture

Eight different textural features were computed over the image using the built-in ENVI function for texture-based co-occurrence filters, which is consistent with Haralick's approach. These eight features are: mean, variance, homogeneity, contrast, dissimilarity, entropy, second moment, and correlation (cf. [12] for the specific formulas). We could show that the entropy – which is a *quantitative measure of the randomness of the grey-level distribution in an image* – is well suited for extraction of avalanche-affected areas, as these areas have high entropy (Fig. 7). Unfortunately, there are other areas with high entropy as well. These areas correspond to sparse forest or areas with large intensity variations due to material changes or shadows.

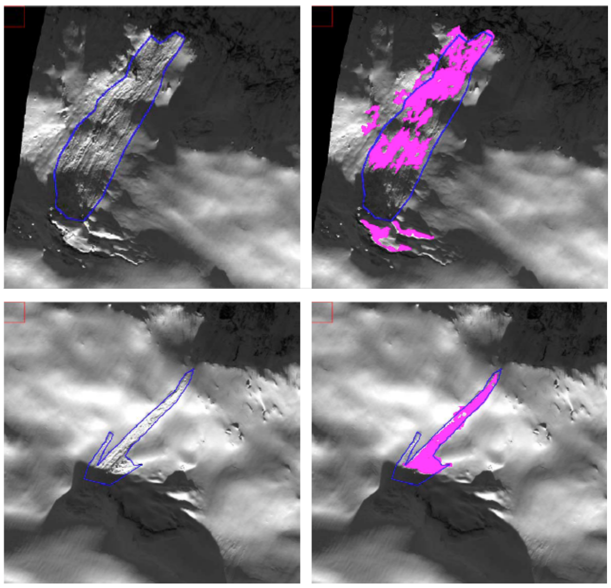

Figure 7. Two avalanches (upper left corner of the Hellesylt image, see Fig. 5) segmented based on texture. Left: avalanches outlined manually in blue on the panchromatic image. Right: high entropy segments are overlain in pink.

4.2. Segmentation based on directional filters

The results of applying a filter bank on various regions are that various image features are enhanced depending on the type of filter applied. Typically, the avalanche is enhanced by applying the aspect directional filters whereas sparse trees are suppressed (Fig. 8). By applying the vertical directional filters, we obtain the opposite response.

Clearly the segmentation algorithm manages to extract areas corresponding to avalanches (Fig. 8), and also manages to correctly segment areas corresponding to sparse trees. Some erroneous areas occur, but it is expected that they can be removed in the classification stage. The segmentation algorithm is not able to fully capture the shape of the avalanches, and some further improvements are necessary in order to fulfil that.

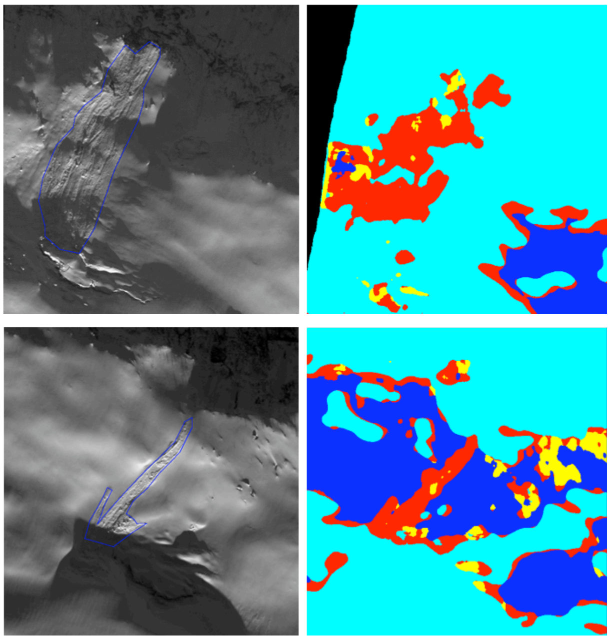

Figure 8. Same avalanches as in Fig. 7, this time segmented with the directional filter approach. Left: avalanches outlined manually in blue on the panchromatic image. Right: red areas correspond to avalanches, blue to rugged snow, yellow to sparse trees, and cyan to rock (respectively shadow, see section 5.2).

Furthermore, the algorithm tends to mix shadowed areas with rock since both classes appear with low intensity values.

The results of applying the directional filter method on the Dalsfjorden image, where the texton dictionary was trained from Hellesylt image, worked well. As for the Hellesylt image, the algorithm extracted areas corresponding to avalanches and managed to separate spares forest and rugged snow from avalanches. Also for the Dalsfjorden image, the algorithm was not able to fully capture the shape of the avalanches. The validation image contained many shadow areas that introduced erroneous classifications.

5. DISCUSSION AND CONCLUSIONS

5.1. Data

Optical data accessible through ESA or ESA TPMs (such as, for example, the here used SPOT-2/-4 data) proves to have insufficient spatial resolution for the purpose of avalanche detection and mapping. This applies especially to the available multi-spectral data, but also, even though to a less pronounced degree, to available panchromatic data. This problem turned out to be inherent for the entire project. The project had, therefore, to rely heavily on VHR data from commercial resellers, in the present case, namely QuickBird imagery.

Detection and mapping by both visual methods as well as by applying automatic detection algorithms worked well for the QuickBird test scenes and yielded very promising results.

Currently, VHR imagery (≤ 2.5 m spatial resolution) is, among others, available on a commercial basis from the following satellites:

- QuickBird (Digital Globe Inc., U.S.A.)
- WorldView-1, WorldView-2 (Digital Globe Inc., U.S.A.)
- Ikonos (GeoEye Inc., U.S.A.; partly through ESA TPM)
- Orbview-1, Orbview-2, Orbview-3, GeoEye-1, GeoEye-2 (GeoEye Inc., U.S.A.)
- SPOT-5 (Spot Image SA, France)
- RapidEye (RapidEye GmbH, Germany)

In addition, new optical satellites become available with increasing frequency.

However, this potential abundance of satellites providing VHR optical imagery shall not conceal the fact that image coverage can be quite scarce for certain regions. This is especially true for regions which are (a) either not in the focus of the commercial satellite image providers (typically, regions not prone to large natural hazards or that do not feature large urban areas, are not within the target area of these entities) and (b) or areas which are located at high latitudes. The latter is especially true during the winter season, due to unfavourable illumination situations at high latitudes during periods with low sun-elevation angle.

Near-real-time avalanche detection and mapping will, therefore, strongly depend on the coincidental availability of such imagery. Operational hind-cast avalanche detection could be effectuated by entering on-demand purchase agreements with one (or several) satellite imagery provider(s). The costs involved in such agreements should, however, not be underestimated. Therefore, image availability is seen as the main bottleneck for the proposed service at present.

5.2. Automatic detection and mapping

The perhaps greatest challenge in order to automatically detect and map avalanche deposits is to perform a successful segmentation, i.e., to locate the image regions that correspond to potential avalanche sites. We could show that both GLCMs and directional filter approaches are able to extract potential avalanche areas. The segmentation results indicate that the GLCM approach extracts the boundaries better than the directional filter approach, but struggles to separate sparse trees from avalanches. The strength of the directional filter approach is that it is able to separate sparse trees from avalanches. The major drawback of this approach is that it often confuses shadowed areas with rock. Some further investigations are needed in order to process shadowed areas successfully.

It should also be considered to combine the two approaches, e.g., to include one or several GLCM features as input to the texton dictionary, and model the database generation steps of the directional filtering approach. By combining the two segmentation approaches some of the texture features produced from the GLCM matrices could be used as input to the directional filter approach.

To extract the shape of the avalanche is a challenging task. A region-growing method is suggested, but research needs to be conducted in order to find suitable criterions on how to grow the avalanche region. The directional filter bank approach applied a model-based classification in order to classify a given pixel to one of the texture types. Other approaches may be better in order to define the regions, for instance, by weighting the pixels in the neighbourhood of the pixel under investigation, or by applying a random field as a means for introducing contextual information.

ACKNOWLEDGEMENTS

The avalRS project is funded by the ESA DUE (Data User Element) Innovator II programme (Contract No. 22139/08/I-EC).

REFERENCES

1. Vallet, J., Skaloud, J., Koelbl, O. & Merminod, B. (2000). Development of a helicopter-based integrated system for avalanche mapping and hazard management. *The International Archives of the Photogrammetry*. Remote Sensing and Spatial Information Sciences 33: 565-572.
2. Sailer, R., Fromm, R., Jörg, P., Schaffhauser, A. & Adams, M. (2008). Ground Based Remote Sensing of Snow Properties and Avalanche Simulation. In: *Proceedings of the International Conference Studying, Modeling and Sense Making of Planet Earth*, Mytilene, Lesvos, Greece, June 1-6, 2008.
3. Wiesinger, T. & Adams, M. (2008). Schnee und Lawinen in den Schweizer Alpen Winter 1998/1999. *SLF report*, Davos.
4. Wiesmann, A., Wegmüller, U., Honikel, M., Strozzi, T. & Werner, C.L. (2001). Potential and methodology of satellite based SAR for hazard mapping. In: *Proceedings of IGARSS 2001*, *Sydney, Australia*, 9–13 July 2001.
5. Wiesmann, A., Strozzi, T., Werner, C., Wegmüller, U. & Santoro, M. (2007). Microwave remote sensing of alpine snow. *IEEE International*: 1223–1227.
6. Rott, H., Cline, D., Nagler, T., Pulliainen, J., Rebhan, H. & Yueh, S. (2007). CoreH_2O – A Dual-Frequency SAR Mission for Hydrology and Climate Research. In: *Proceedings of the IGARSS 2007 Barcelona, Spain,* July 23-27.
7. Bühler, Y., Hüni, A., Christen, M., Meister, R. & Kellenberger, T. (2009). Automated detection and mapping of avalanche deposits using airborne optical remote sensing data. *Cold Regions Science and Technology*, doi:10.1016/j.cold regions.2009.02.007.
8. Solberg, A., Brekke C. & Husøy, P. (2007). Oil spill detection in Radarsat and Envisat SAR images. *IEEE Trans. Geosci. Remote Sens*. 45: 746-755.
9. Trier, Ø.D., Larsen, S.Ø. & Solberg, R. (2009). Automatic detection of circular structures in high-resolution satellite images of agricultural land. *Archaeological Prospection* 16: 1-15.
10. Larsen, S.Ø., Koren, H. & Solberg, R. (2009). Traffic Monitoring Using Very-High-Resolution Satellite Imagery. *Photogrammetric Engineering and Remote Sensing* 75: 859-869.
11. Larsen, S.Ø., Salberg, A.-B. & Solberg, R. (2010). Automatic detection of avalanches in high-resolution optical satellite data. Results from the ESA aval-RS project's feasibility study on automated avalanche detection. Norwegian Computing Center, internal report no. SAMBA/04/10, May 21st, 2010: 38 pp.
12. Haralick, R.M., Shanmugam, K. & Dinstein, I. (1973). Textural Features for Image Classification. *IEEE Trans. Systems, Man, Cybern*. 3(6): 610-621.
13. Bovik, A.C., Clark, M. & Geisler, W.S. (1990). Multichannel texture analysis using localized spatial filters. *IEEE Trans. Pattern Anal. Machin. Intell.* 12(1): 55-72.
14. Jain, A.K., Ratha, N.K. & Lakshmanan, S. (1997). Object detection using Gabor filters. *Pattern Recogn.* 30(2): 293-309.
15. Varma, M. & Zisserman, A. (2004). A statistical approach to texture classification from single images. *Int. J. Computer Vision: Special Issue on Texture Analysis and Synthesis* 62(1-2): 61-81.